Discovery of potent trifluoromethyl acrylamide warhead-containing inhibitors against a cysteine-based enzyme

臺北醫學大學藥學系

黃偉展博士

黃偉展 博士

- 2024/01 迄今-臺北醫學大學藥學院副院長
- 2019/08 迄今-臺北醫學大學藥學系教授
- 2017/08 迄今-臺北醫學大學生藥學研究所教授
- 2011/08 至2017/07-臺北醫學大學生藥學研究所副教授
- 2007/08 至2011/07-臺北醫學大學生藥學研究所助理教授

研究專長
- 有機合成
- 藥物化學
- 循理性藥物設計
- 天然物化學

研究主題
Development of selective histone deacetylase inhibitors
Design of kinase inhibitors targeting idiopathic pulmonary fibrosis
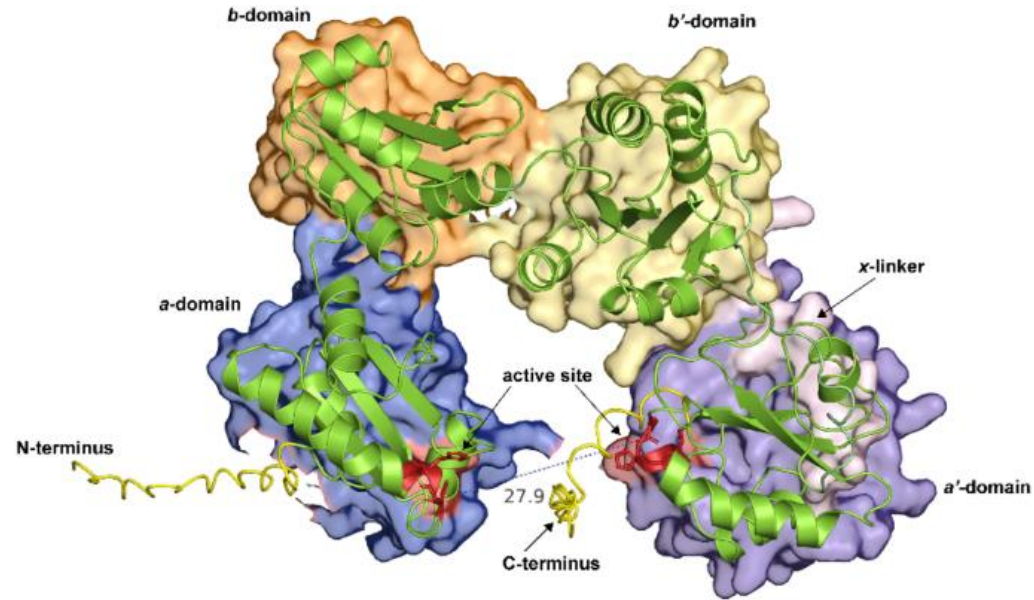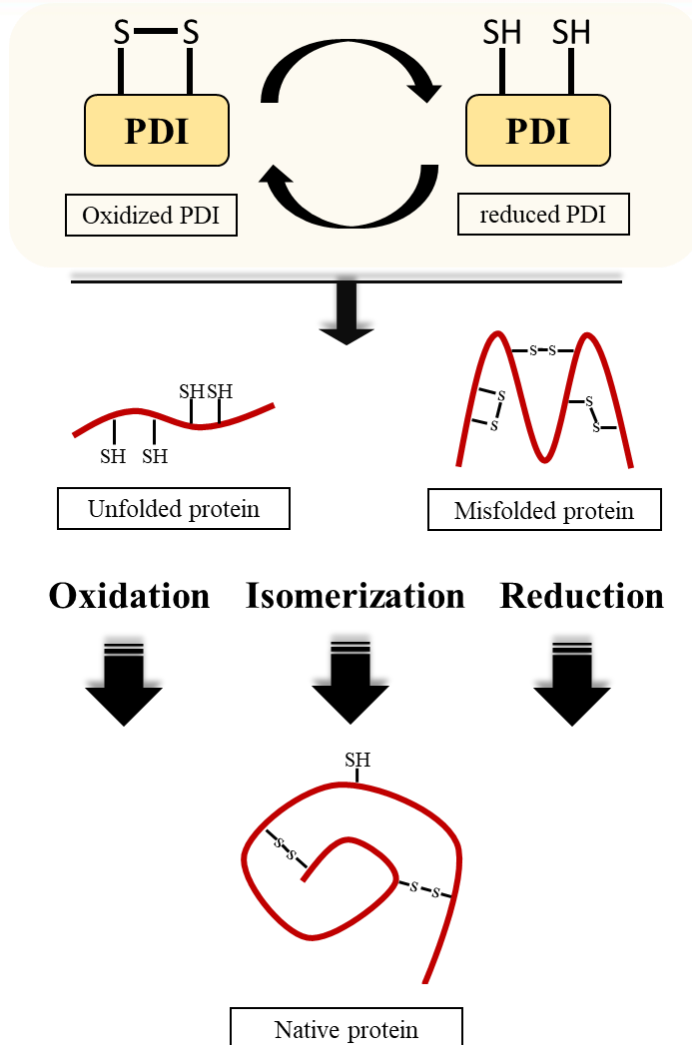Natural product-inspired drug development

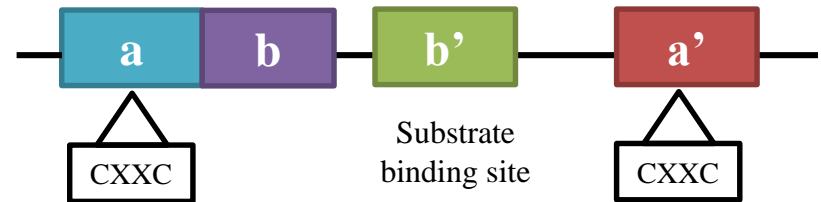**聯絡資訊**
Email: wjhuang@tmu.edu.tw
Phone: 02-27361661 #6152
Office:臺北醫學大學藥學暨營養大樓10F1017室

Protein disulfide isomerases (PDIs)

Cell & Bioscience (2022) 12:129

Classification of PDIs

- The 21 members of PDI family regulate multiple biological function in various tissue due to difference of localization, structure, enzyme property and substrate specificity.

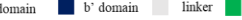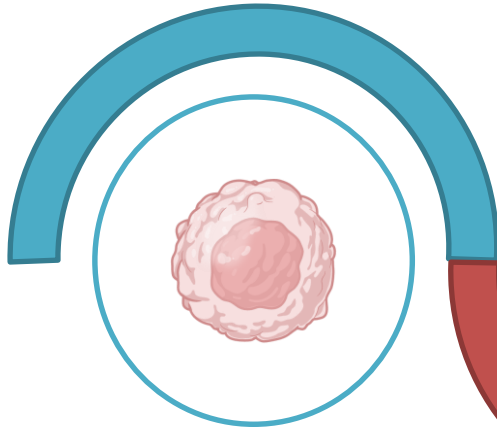| Protein name	Domain composition	Subcelluar location	Amino acids
PDIA1		Endoplasmic reticulum Extracellular space Plasma membrane Cytosol	508
PDIA2		Endoplasmic reticulum	525
PDIA3		Endoplasmic reticulum Extracellular space Nucleus	505
PDIA4		Endoplasmic reticulum Extracellular space	645
PDIA5		Endoplasmic reticulum	519
PDIA6		Endoplasmic reticulum Extracellular space Plasma membrane Cytosol	440
PDIA7		Endoplasmic reticulum	584
PDIA8		Endoplasmic reticulum	273
PDIA9		Endoplasmic reticulum	261
PDIA10		Endoplasmic reticulum Extracellular space	406
PDIA11		Endoplasmic reticulum	280
PDIA12		Endoplasmic reticulum Mitochondrion	296
PDIA13		Endoplasmic reticulum Plasma membrane	454
PDIA14		Endoplasmic reticulum Nucleus	349
PDIA15		Endoplasmic reticulum Extracellular space Lysosome	432
PDIA16		Endoplasmic reticulum	172
PDIA17		Endoplasmic reticulum Extracellular space	175
PDIA18		Endoplasmic reticulum	166
PDIA19		Endoplasmic reticulum	793
PDIB1		Endoplasmic reticulum Mitochondrion	396
PDIB2		Endoplasmic reticulum	399

NH$_2$-terminal   a type domain   b domain   b' domain   linker   Ca$^+$ binding domain   ER retention sequence   Transmembrane domain

TAIPEI MEDICAL UNIVERSITY

Overexpression of PDIs in various disease

Cardiovascular disease

- **Thrombosis**
- Atherogenesis

Fibrosis-related disease

- Lung fibrosis
- Kidney fibrosis
- Heart fibrosis
- Liver fibrosis

Cancer

- Breast cancer
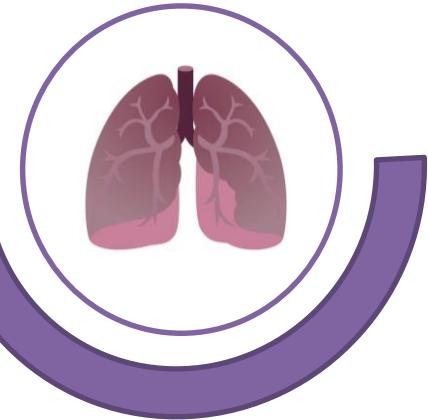- Multiple myeloma
- Ovarian cancer
- **Glioblastoma multiforme**
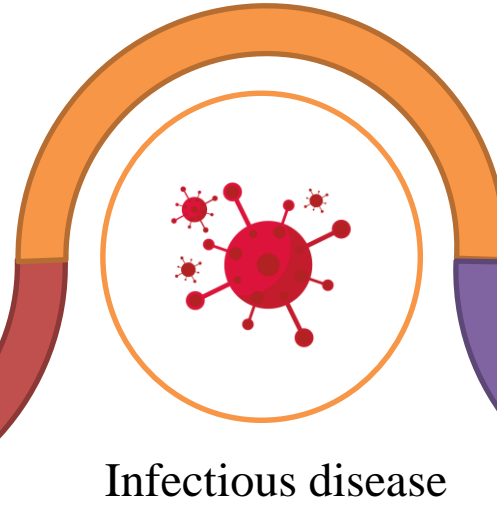
Infectious disease

- Influenza A and B virus
- Human immunodeficiency virus 1 (HIV-1)
- Dengue virus (DENV)

The role of PDI in thrombus
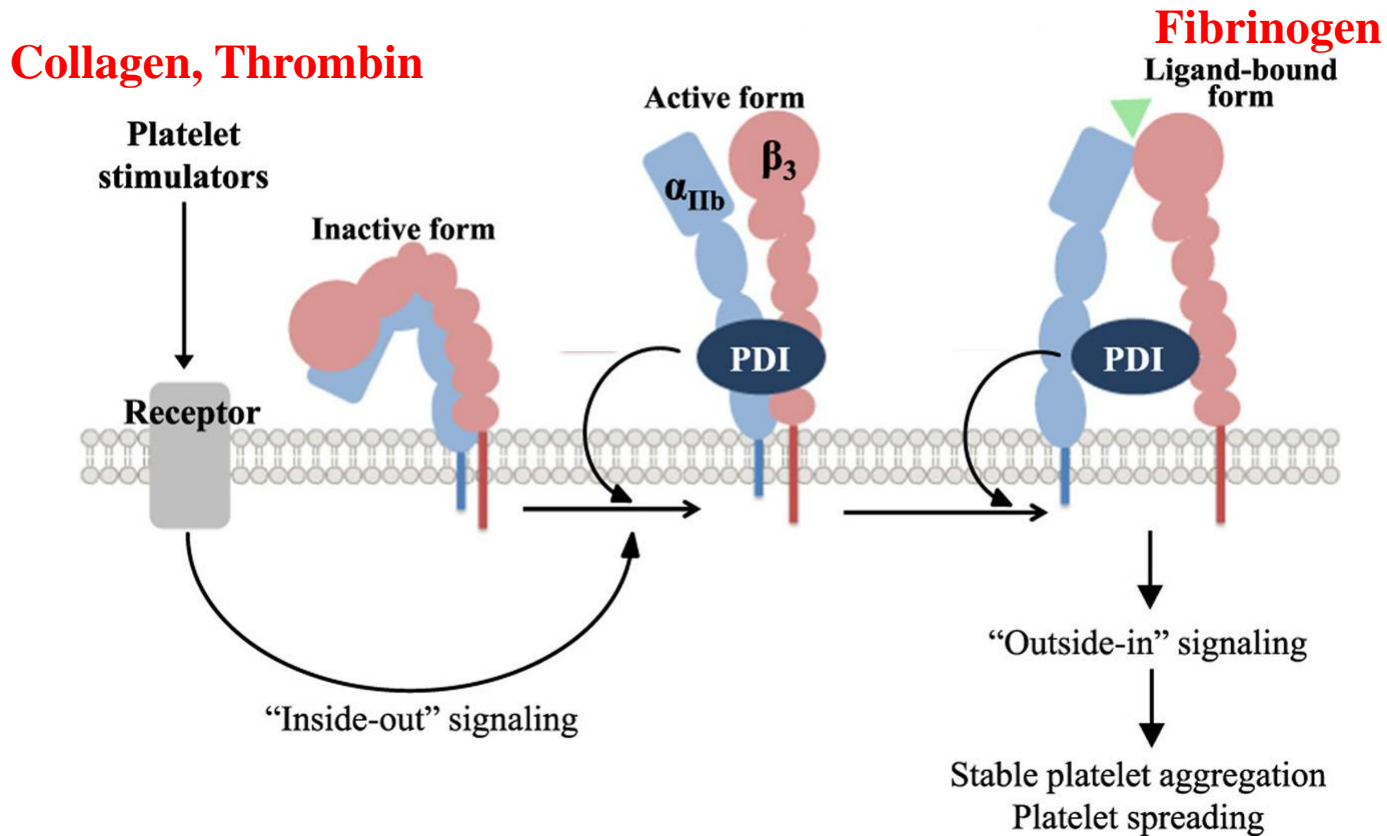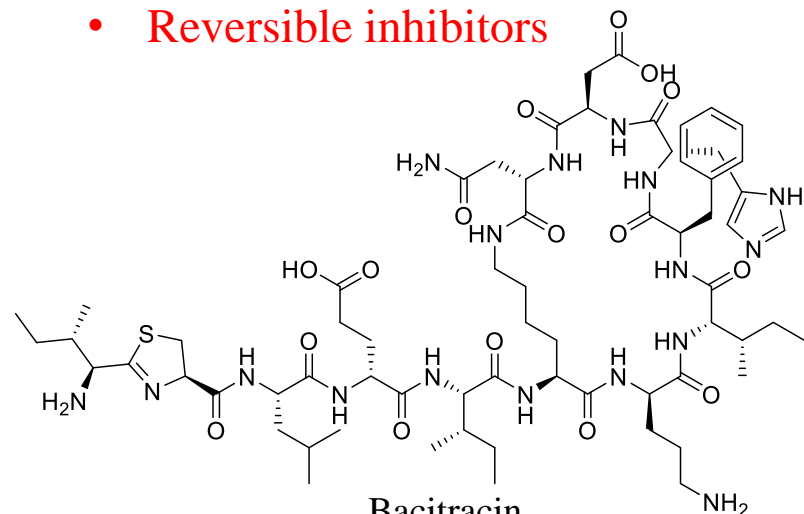
- Inhibition of PDI decreases platelet thrombus and fibrin formation in a mouse model of laser-induced cremaster arteriolar injury. J Clin Invest 2008, 118, 1123-31

- Loss of platelet PDI in megakaryocyte-specific PDI CKO mice leads to weak activation of αIIbβ3 integrin after agonist stimulation, resulting in reduced platelet thrombus formation in vivo. J Clin Invest 2015, 125, 4391-406

- Tail bleeding time and blood loss did not significantly increase in platelet-specific PDI–deficient mice, compared with control mice. Blood. 2013 Aug 8; 122(6): 1052–1061.

- Mice treated with myricetin displayed similar bleeding time when compared to vehicle control.
  Front. Pharmacol., 31 January 2020

Platelet aggregation

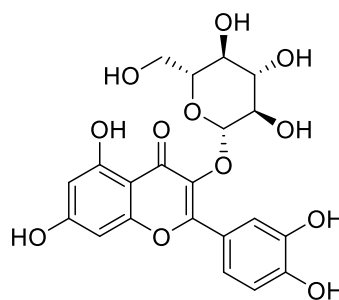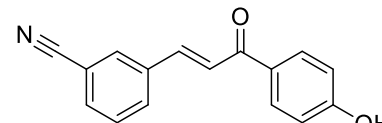**Collagen, Thrombin**

Fibrinogen
Ligand-bound form

Platelet stimulators

Inactive form

Active form

β_3

α_{IIb}

PDI

PDI

Receptor

"Inside-out" signaling

"Outside-in" signaling

Stable platelet aggregation
Platelet spreading

PDI inhibitors

- Reversible inhibitors
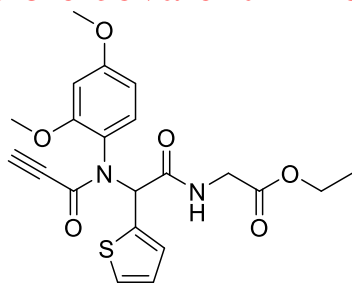
Bacitracin
PDI = 150-200 μM
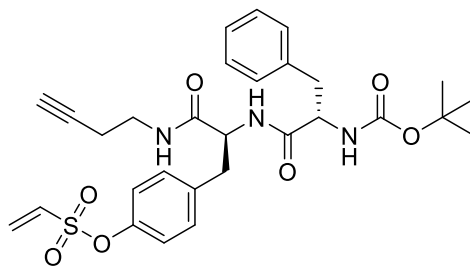
Isoquercetin
PDI = 6 μM

BAP2
PDI = 0.9 μM
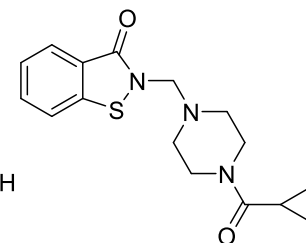
LOC14
PDI = 5 μM

- Irreversible covalent inhibitors

PACMA31
PDI = 30.2 μM

P1
PDI = 1.7 μM
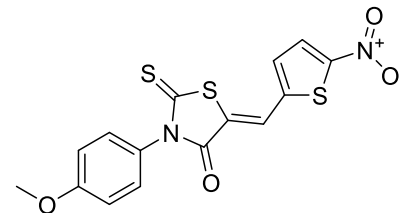
CCF-642
PDI = 2.9 μM
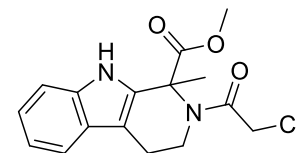
16F16
PDI = 70 μM

Covalent inhibitor
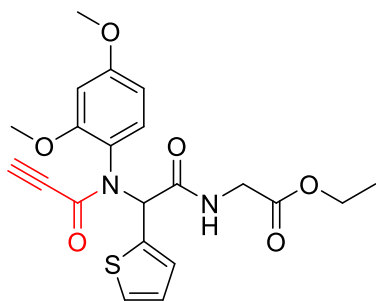
PACMA31
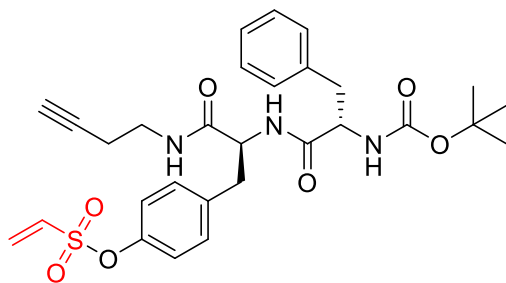
P1
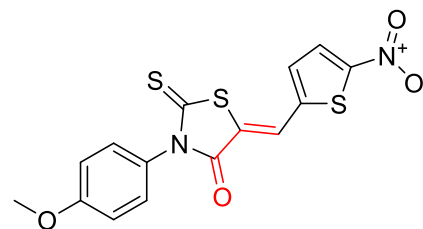
CCF-642
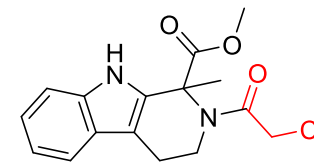
16F16

Michael addition
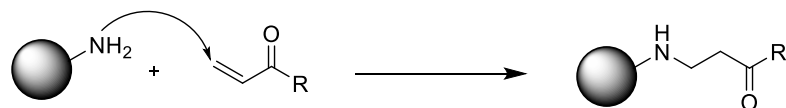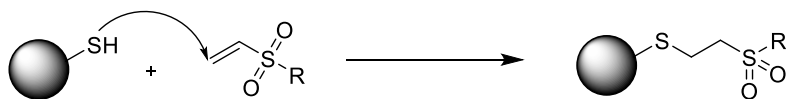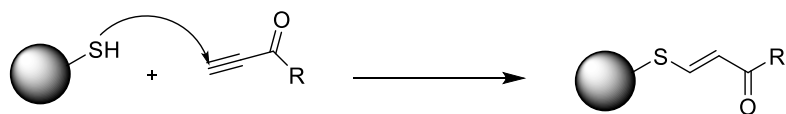
Nucleophilic substitution

Drug design

Warhead

High toxicity
Weak metabolic stability

CPD
PDI IC$_{50}$=1.6 μM

2a-f, **3-4**, **7**

2d
PDI IC$_{50}$=2.2 μM

R=

14d
PDI IC$_{50}$=480 nM

9a-d, **12**, **14a-d**

台北醫學大學
TAIPEI MEDICAL UNIVERSITY
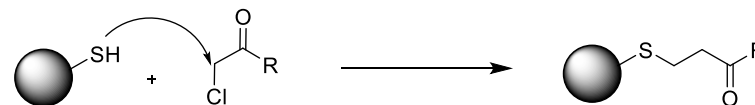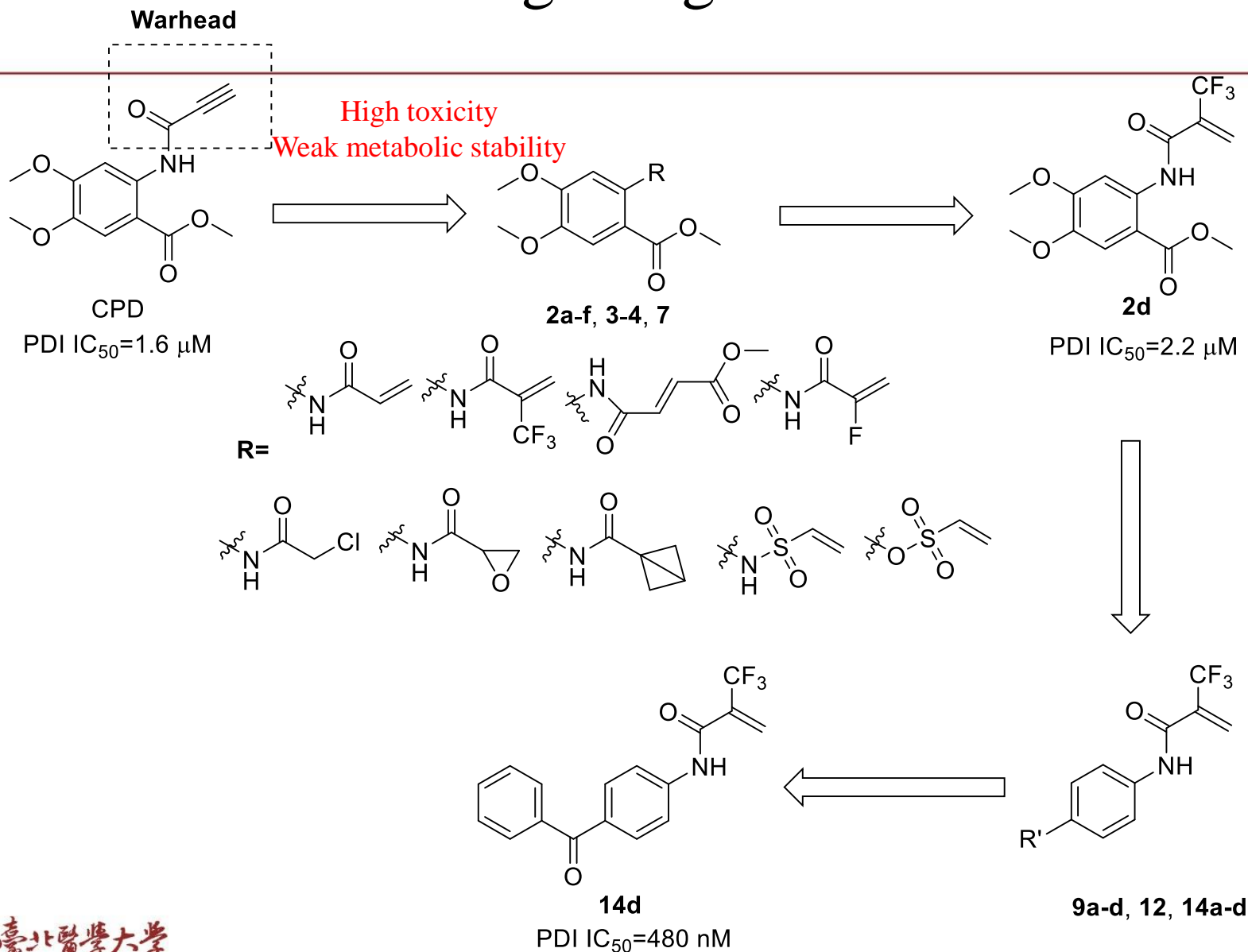
Results and discussion

Chemistry

Scheme 1 Reagents and condition: (**a**) RCOCl or RCOOH, EDCI, DMAP, DCM; (**b**) K_2CO_3, 37% H_2O_2, THF/H_2O; (**c**) RCOOH, LIHMDS, THF
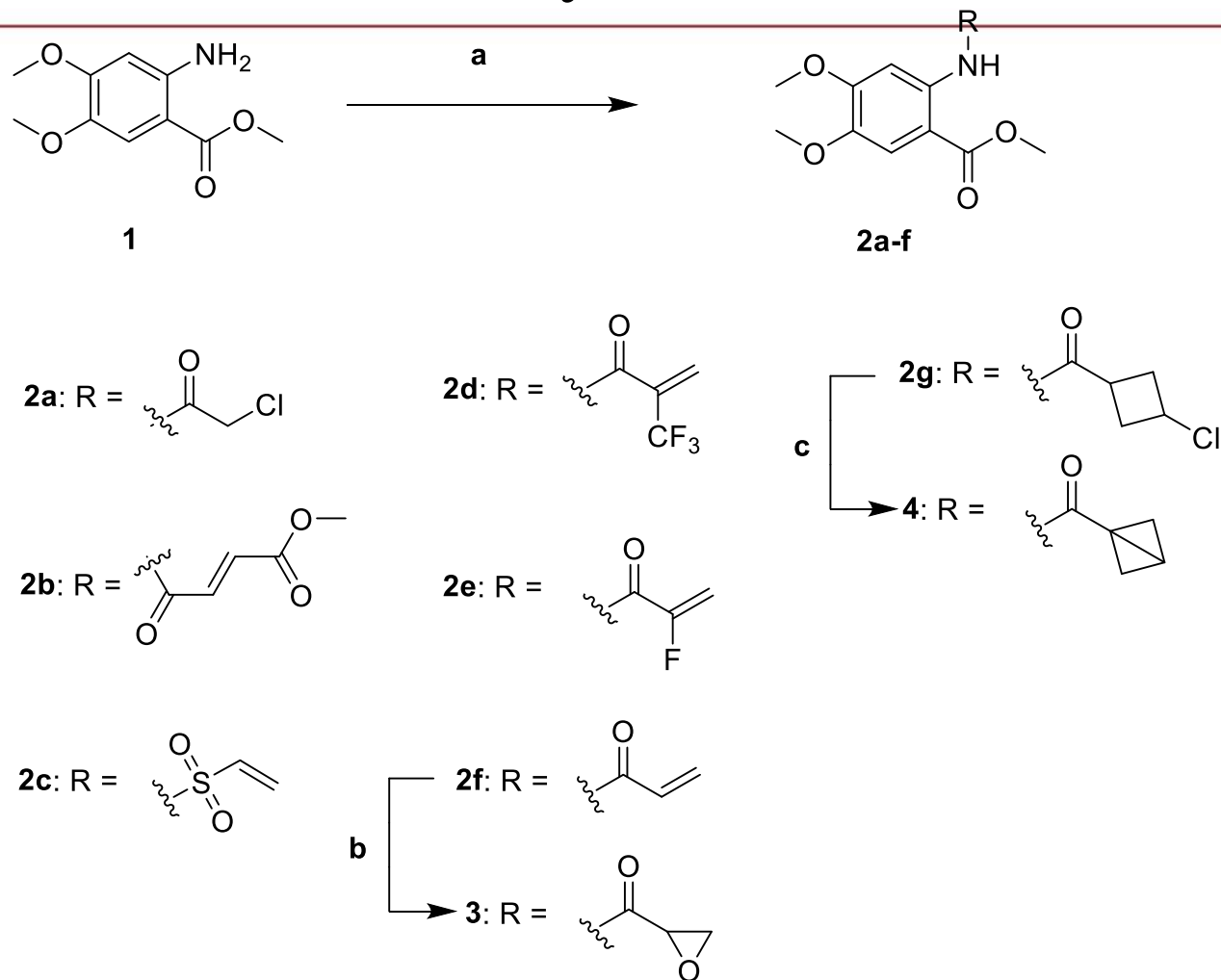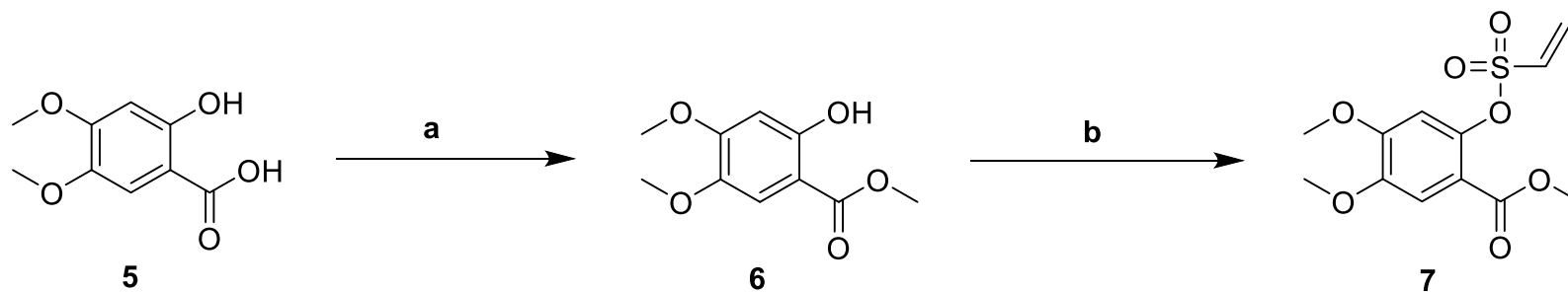
Chemistry

Reagents and conditions: (**a**) H_2SO_4, MeOH, Δ; (**b**) 2-chloroethane-1-sulfonyl chloride, Et_3N, CH_2Cl_2

Chemistry
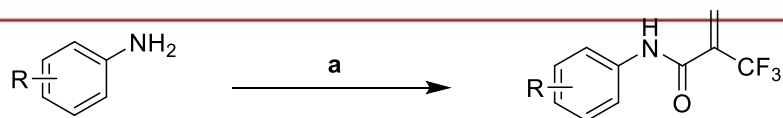
8a: R = 3,4-DiOMe
8b: R = 3,4,5-TriOMe
8c: R = 4-CF$_3$
8d: R = 4-*t*-butyl

9a: R = 3,4-DiOMe
9b: R = 3,4,5-TriOMe
9c: R = 4-CF$_3$
9d: R = 4-*t*-butyl

10   **11**   **12**

13a-d   **14a-d**

R'=

a   b   c   d

Reagents and conditions: (**a**) 2-Trifluoromethylacrylic acid, EDCI, DMAP, DCM; (**b**) PhB(OH)$_2$, Pd(OAc)$_2$, K$_2$CO$_3$, DMF-H$_2$O, Δ
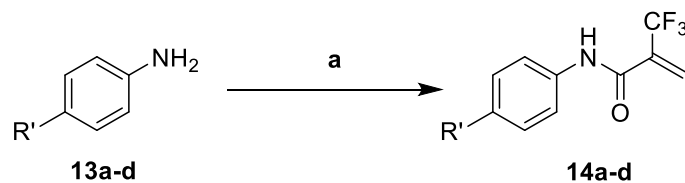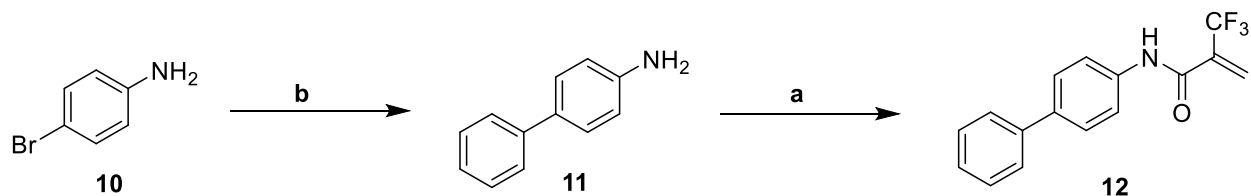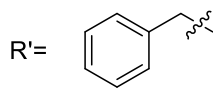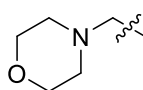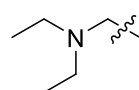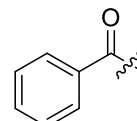
Table 1. IC_{50} values (nM) of enzyme inhibition of compounds **2a-f**, **3-4**, **7** against PDIA1

2a-f, 3-4, 7
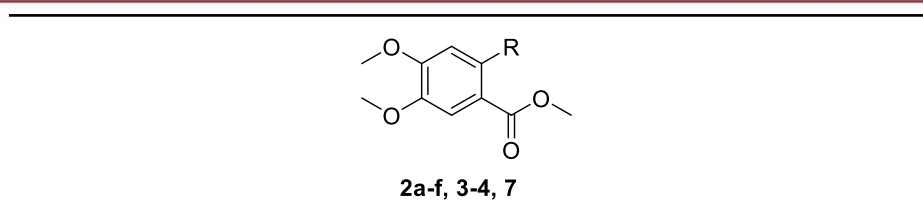
Compound	IC_{50}
2a	>40000
2b	>40000
2c	18800
2d	2200
2e	>40000
2f	>40000
3	>40000
4	>40000
7	1100
CPD	1600

2a: R =

2b: R =

2c: R =

2d: R =

2e: R =

2f: R =

3: R =

4: R =

7: R =

臺北醫學大學
TAIPEI MEDICAL UNIVERSITY
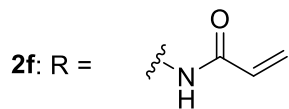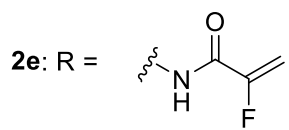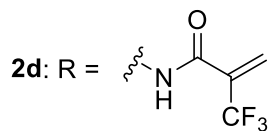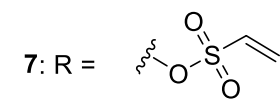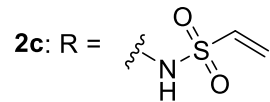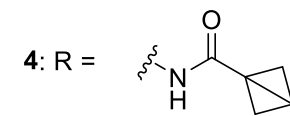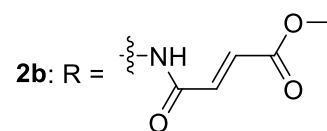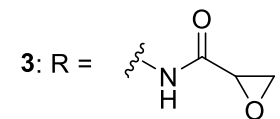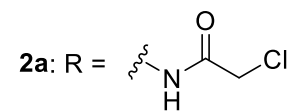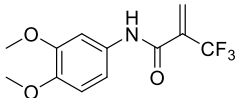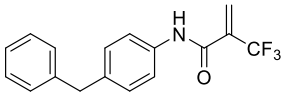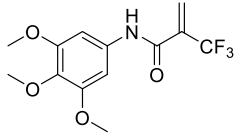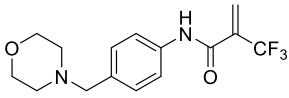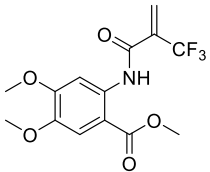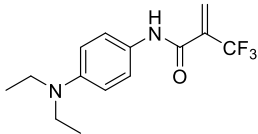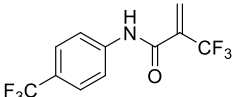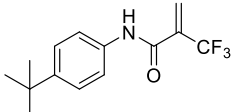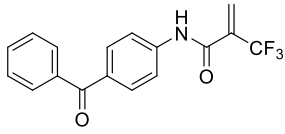
Table 2. IC_{50}[a] values (nM) of enzyme inhibition of compounds **9a-d, 12** and **14a-d** against PDIA1

Compound	IC_{50}
9a	3000 ± 500
9b	580 ± 57
9c	680 ± 21
9d	870 ± 16
12	1630 ± 280
14a	560 ± 16
14b	1210 ± 48
14c	840 ± 45
14d	480 ± 4

[a] Data are provided from three independent experiments.

2d

PDIA1 IC_{50}: 2200 nM
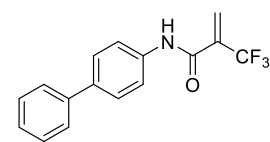
Compound **14d** is identified as a reversible covalent PDI inhibitor

(A)

PACMA31

- DMSO
- PACMA31 4µM (10X dilution from 40µM)
- PACMA31 40µM
- PACMA31 4µM

(B)

14d

- DMSO
- 14d 0.2µM (10X dilution from 2µM)
- 14d 2µM
- 14d 0.2µM
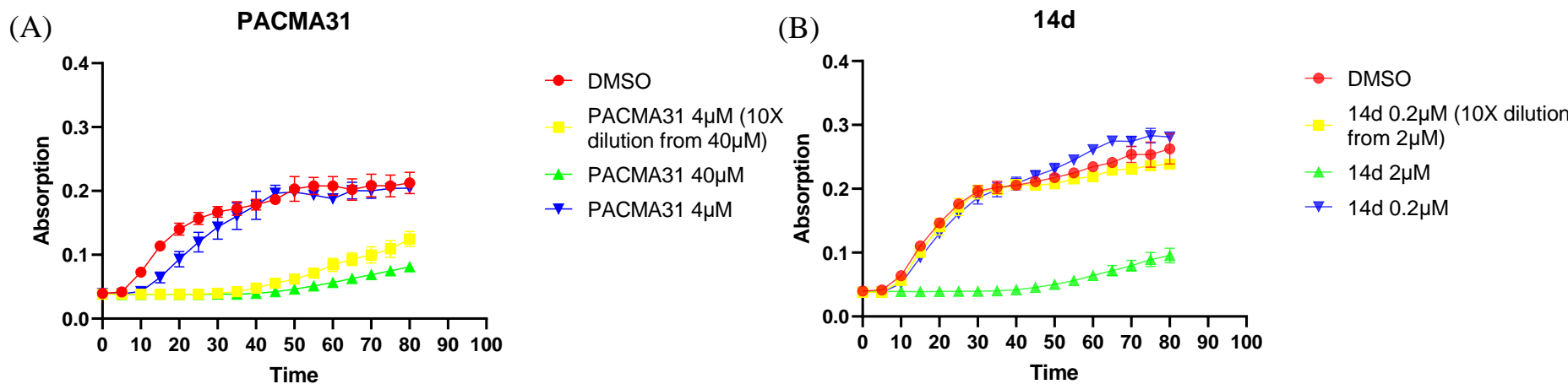
Figure 1. Reversibility of compound 14d inhibition of PDI (A) Pre-incubation of PCAMA 31 (40 µM) with recombinant PDI were diluted 10-fold with buffer (yellow). The PDI inhibitory activity was determined to compare with samples containing PDI in the absence (red) or presence of 4 µM (green) or 40 µM (blue) PACMA31. (B) Pre-incubation of **14d** (2 µM) with recombinant PDI were diluted 10-fold with buffer (yellow). The PDI inhibitory activity was determined to compare with samples containing PDI in the absence (red) or presence of 0.2 µM (green) or 2 µM (blue) **14d**.

- The computed proton affinity of the corresponding carbanions, suggesting that the acidity of the proton at the α-position of the adduct provides the driving-force for the β-elimination.

J. Am. Chem. Soc. 2014, 136, 36, 12624–12630

retro-Michael reaction
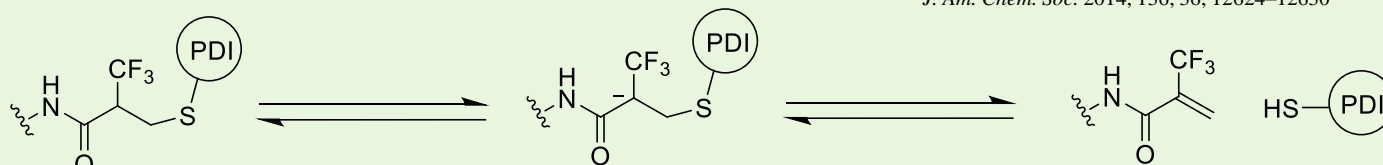
Molecular modeling analysis of compound **14d** against PDIA1
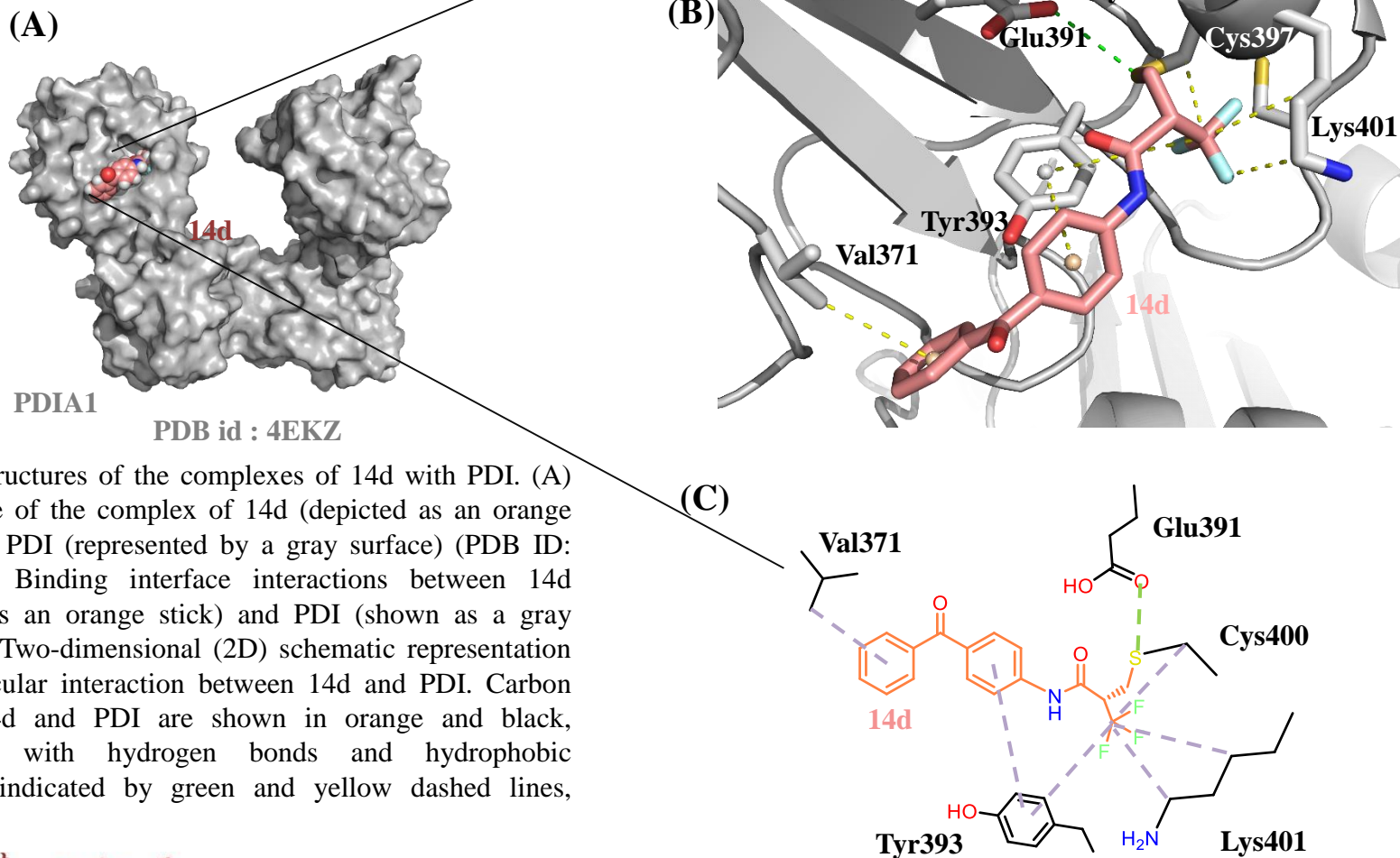
Figure 2. Structures of the complexes of 14d with PDI. (A) The structure of the complex of 14d (depicted as an orange sphere) with PDI (represented by a gray surface) (PDB ID: 4EKZ). (B) Binding interface interactions between 14d (illustrated as an orange stick) and PDI (shown as a gray ribbon). (C) Two-dimensional (2D) schematic representation of the molecular interaction between 14d and PDI. Carbon atoms in 14d and PDI are shown in orange and black, respectively, with hydrogen bonds and hydrophobic interactions indicated by green and yellow dashed lines, respectively.

Compound **14d** exhibited PDIA1 selectivity over other isoform enzymes

Table 3. IC_{50}[a] values (µM) of enzyme inhibition of compounds **14d** and PACMA31 against PDIA3 and PDIA6

14d
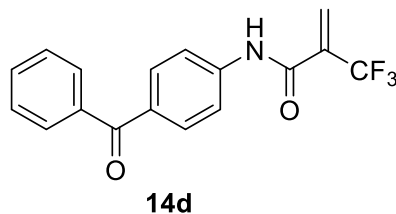
Compound	PDIA1 (PDI)	PDIA3 (ERp57)	PDIA6 (ERp5)
12g	0.48 ± 0.004	1.52 ± 0.01	7.10 ± 2.21
PACMA31	12.4	28.09 ± 1.94	>40

a Data are provided from three independent experiments.

Compound **14d** significantly inhibited platelet aggregation
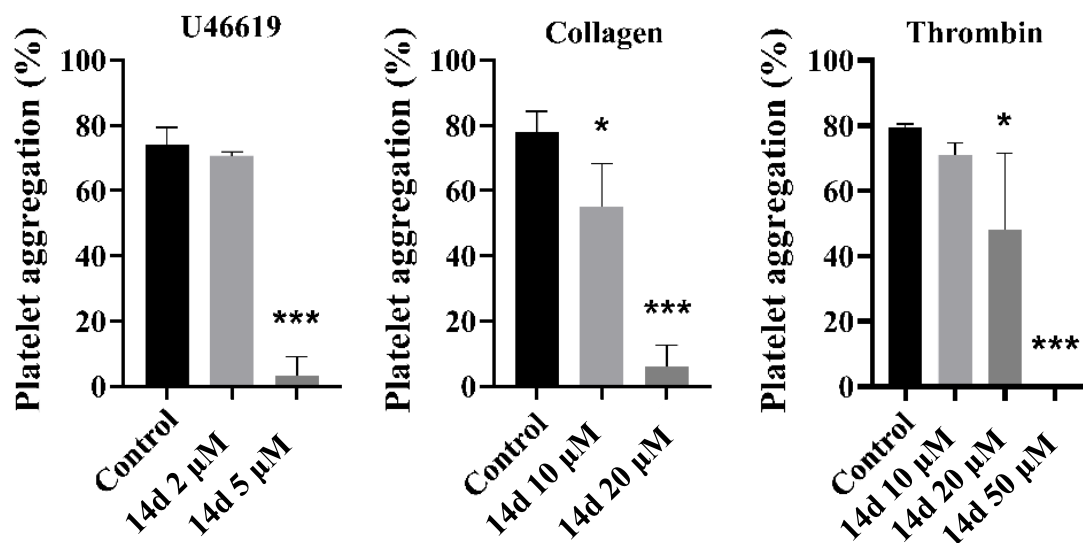
Figure 3. Effects of **14d** on human platelet aggregation. Washed human platelets were incubated with DMSO or **14d** (2 – 50 μM) for 3 min, and then platelet aggregation was induced by U46619 (1 μM), collagen (5 μg/ml) or thrombin (0.05 U/ml). Results were obtained in three independent experiments (mean $\pm$ SEM). *P < 0.05 or ***p < 0.001 as compared with control.

Table 4. IC_{50}[a] values (μM) of anti-platelet aggregation of compounds **14d**

	U46619	**Collagen**	**Thrombin**
14d	3.5 ± 0.1	13.0 ± 1.4	25.5 ± 6.8

a Data are provided from three independent experiments.

Compound **14d** remarkably inhibited GPIIb/IIIa activation and P-selectin expression
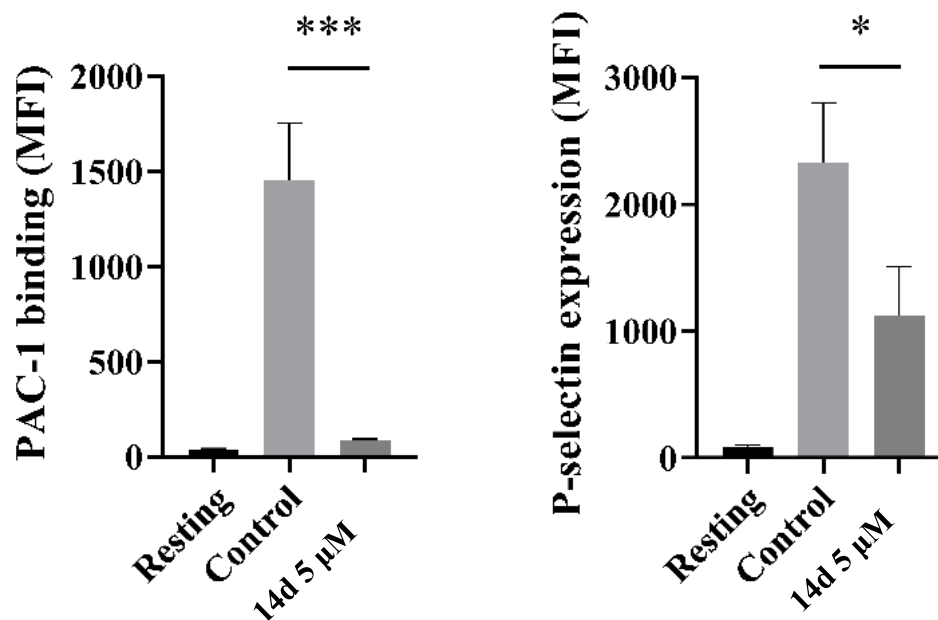
Figure 4. Effects of **14d** on GPIIb/IIIa activation and P-selectin expression. Washed human platelets were incubated with DMSO or **14d** (5 μM) for 3 min, and then stimulated with U46619 (1 μM) for another min. The expressions of active form of GPIIb/IIIa (A) and P-selectin (B) on the cell surface of platelets were determined using flow cytometry with PAC-1-FITC and anti-CD62P-PE antibodies respectively. Results were obtained in three independent experiments (mean ± SEM). *$P < 0.05$ or ***$p < 0.001$ as compared with control.

Compound **14d** significantly reduced *in vitro* thrombus formation

Figure 5. Effects of **14d** on *in vitro* thrombus formation. Human whole blood was incubated with DMSO or **14d** (5 µM) in the presence of DiOC6(3) (1 µM), and then perfused through a collagen-coated flow chamber at a shear rate of 1500 s-1 for 4 min. The coverage areas of thrombi on the collagen-coated surfaces are presented as percentage of control values (n = 3). ***$P < 0.001$ as compared with control.
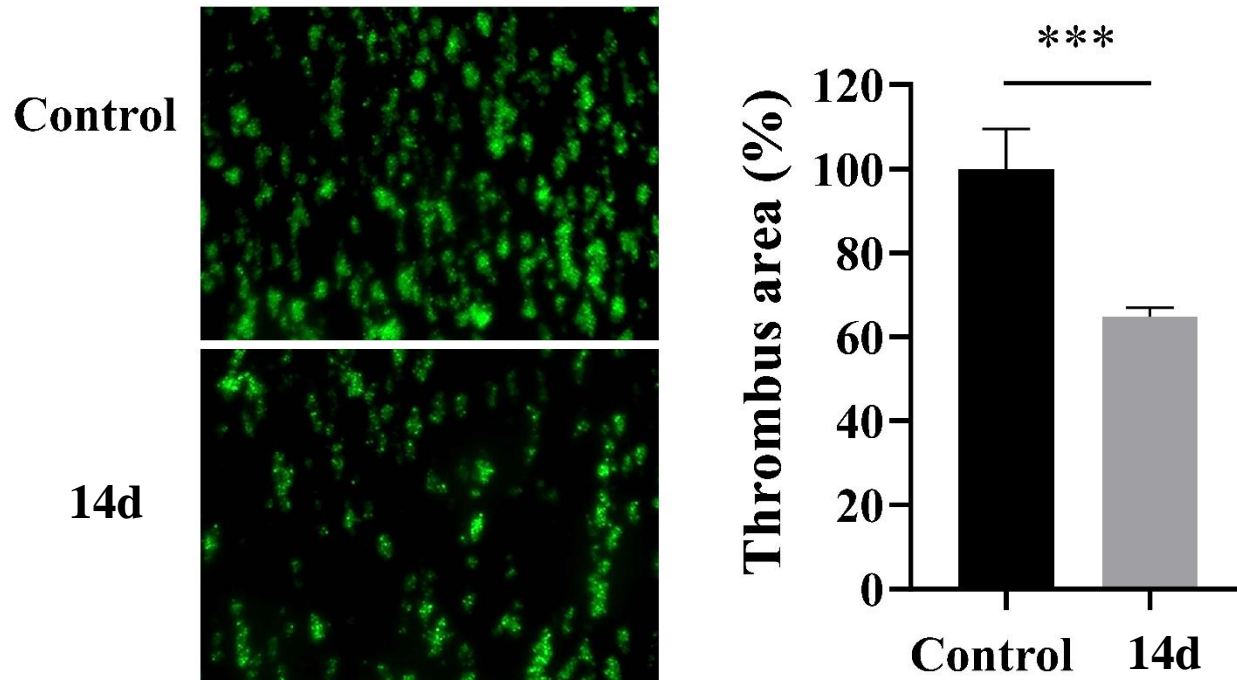
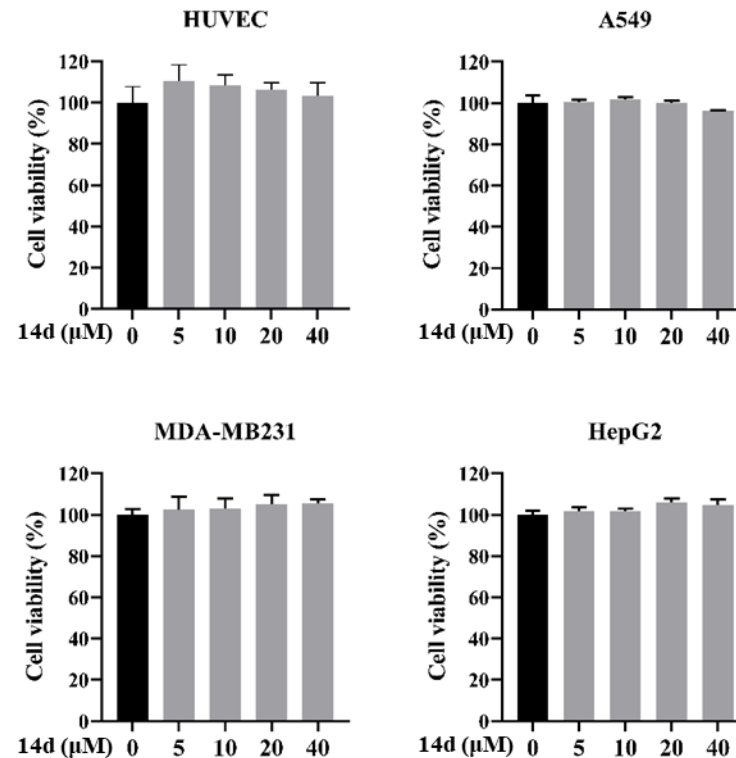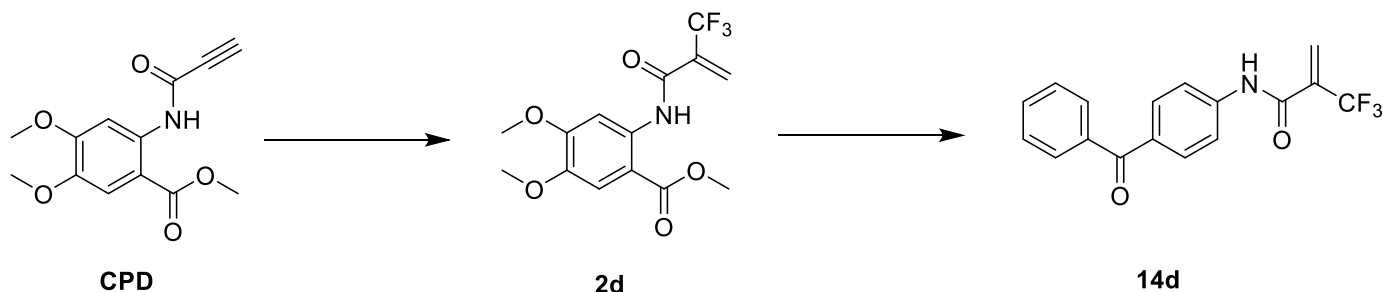# Compound **14d** exhibited low cytotoxicity

Figure 6. Cytotoxicity assay of **14d**. HUVECs or cancer cells (A549, MDA-MB- 231, and HepG2) were incubated with DMSO or **14d** (5 – 40 μM) for 24 h, and then cell viability was determined using MTT assay. Results were obtained in at least three independent experiments (mean ± SEM).
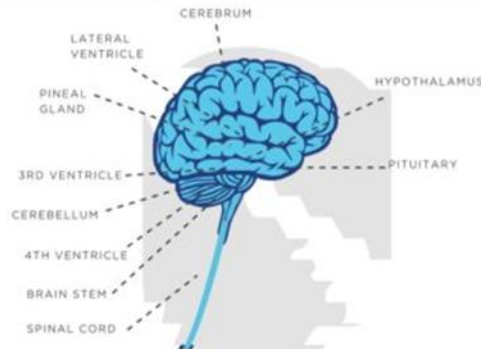
Conclusion

CPD → 2d → 14d

- Trifluoromethyl-acrylamide was an acceptable Michael acceptor for the design of PDI inhibitors.

- Compound **14d** showed considerable PDI inhibitory activity with an IC_{50} value of 480 ± 4 nM.

- The reversibility assay revealed that compound **14d** reversed the formation of the covalent bond with PDIA1, which was presumed to be due to retro-Michael addition.

- Compound **14d** remarkably reduced platelet aggregation and thrombus formation via inhibiting activation of GPIIb/IIIa.

- Compound **14d** show extremely weak cytotoxicity against HUVECs and three human cancer cell lines

Glioblastoma multiforme (GBM)

Glioblastoma multiforme (GBM)

GLIOBLASTOMA AT-A-GLANCE

GLIOBLASTOMA MULTIFORME (GBM), A TYPE OF CENTRAL NERVOUS SYSTEM CANCER, IS THE MOST COMMON AND MOST AGGRESSIVE FORM OF PRIMARY BRAIN CANCER.

COMMON BRAIN CANCER RISK FACTORS

RADIATION EXPOSURE — FAMILY HISTORY — SOME GENETICALLY INHERITED SYNDROMES — MALE GENDER — ADULTS AGES 45-65

SIGNS & SYMPTOMS

THE SIGNS AND SYMPTOMS OF GBM CAN VARY DEPENDING ON THE SIZE AND LOCATION OF THE TUMOR IN THE BRAIN. THE FOLLOWING ARE COMMON SYMPTOMS:

- HEADACHE
- BLURRED VISION
- BALANCE PROBLEMS
- SEIZURES
- NAUSEA
- VOMITING
- DROWSINESS
- WEAKNESS ON ONE SIDE OF THE BODY
- MEMORY AND/OR SPEECH DIFFICULTIES

POTENTIAL & AVAILABLE TREATMENT OPTIONS

TREATMENT OPTIONS FOR GBM VARY DEPENDING ON A NUMBER OF FACTORS—TUMOR SIZE, POSITION, WHETHER IT HAS SPREAD TO OTHER REGIONS OF THE BRAIN AND THE OVERALL HEALTH OF THE PATIENT. SEVERAL TYPES OF TREATMENT MAY BE CONSIDERED BY A HEALTH PROFESSIONAL TO TREAT THIS TYPE OF CANCER, INCLUDING:
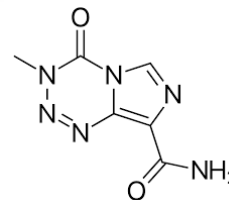
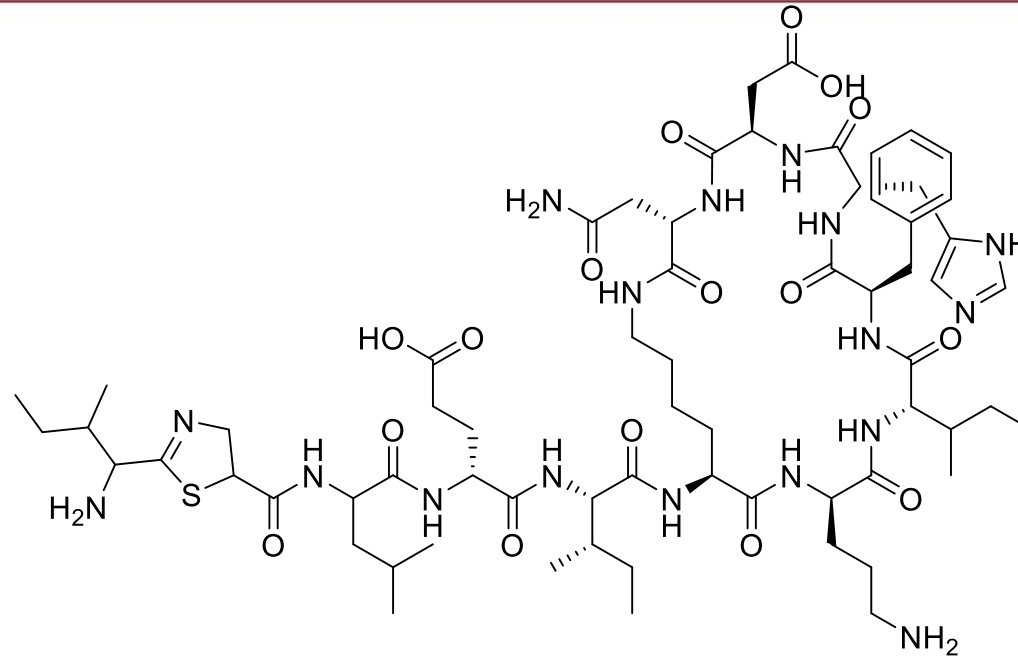SURGERY — RADIATION THERAPY — CHEMOTHERAPY — TARGETED THERAPY — IMMUNOTHERAPY

© 2019 Bristol-Myers Squibb Company
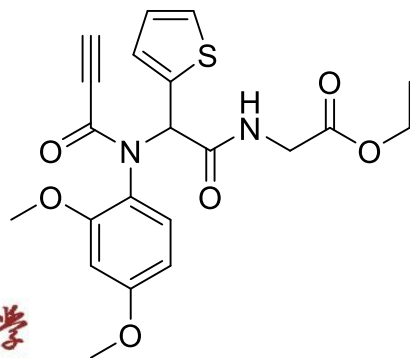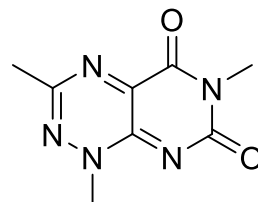
Bristol-Myers Squibb

Temolozomide (TMZ)

26

PDI inhibitors with anti-GBM activity

Bacitrcin

PACMA31

35G8

BAP2

Drug design

9a
PDIA1: 3 µM

22a-c, 27a-b

27a
PDIA1: 0.87 ± 0.02 µM

32a-d, 35a-c, 40

40
PDIA1:0.63 ±0.01µM
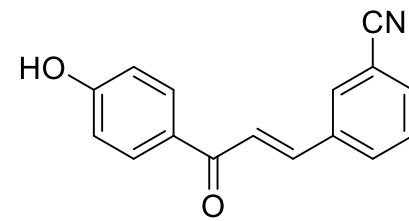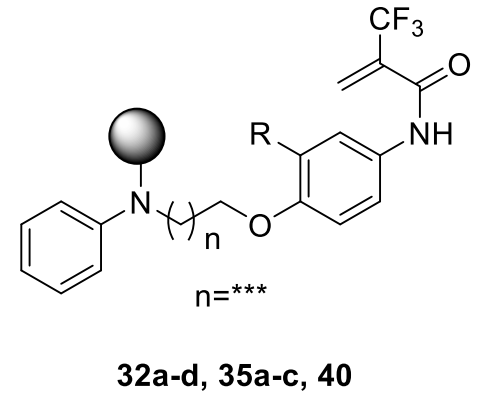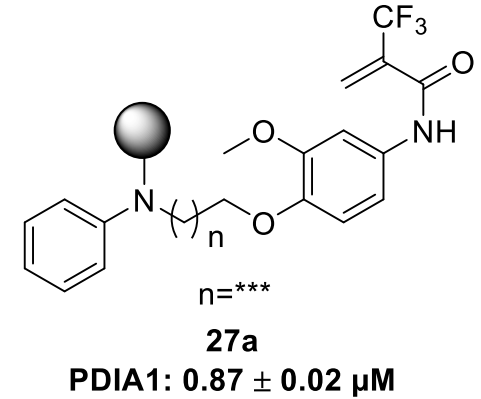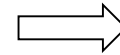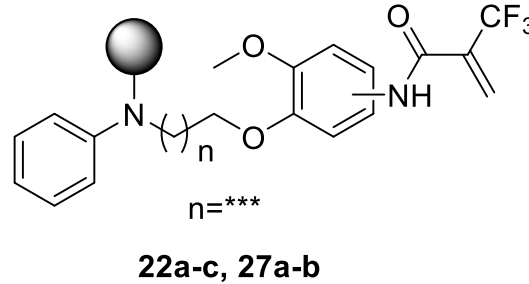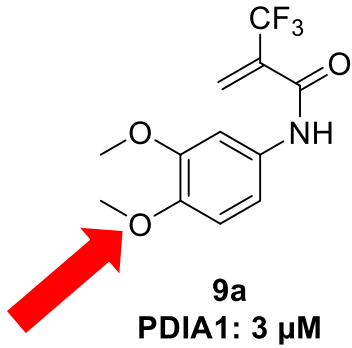
Results and discussion

Table 5. The IC_{50}[a] values (μM) of enzyme inhibition of compound **22a-c**, **27a-b**, **30a-d**, **35a-c**, **40** and PACMA31 against PDI
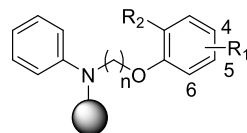
22a-c, **27a-b**, **30a-d**, **35a-c**, **40**

R_1 = 2-(trifluoromethyl)acrylamide (E)

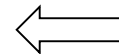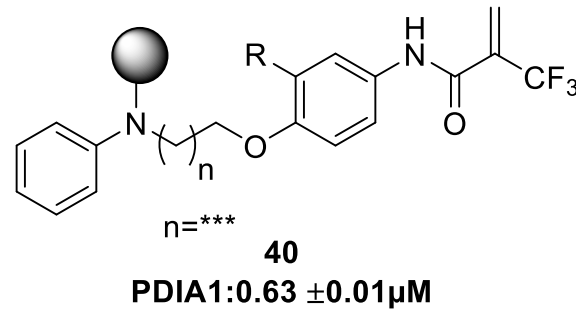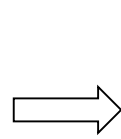| Compound	n	R_1	R_2	PDI
22a	*	4-E	***	0.94 ± 0.04
22b	*	5-E	***	1.00 ± 0.13
22c	*	6-E	***	1.82 ± 0.00
27a	*	4-E	***	0.87 ± 0.02
27b	*	4-E	***	0.98 ± 0.13
30a	*	4-E	***	0.91 ± 0.30
30b	*	4-E	***	1.29 ± 0.03
30c	*	4-E	***	1.56 ± 0.13
30d	*	4-E	***	0.94 ± 0.01
35a	*	4-E	***	0.90 ± 0.02
35b	*	4-E	***	0.98 ± 0.38
35c	*	4-E	***	0.80 ± 0.09
40	*	4-E	***	0.63 ± 0.01
PACMA31				8.10 ± 0.90

[a] Data are provided from three independent experiments.

Table 6. IC_{50}[a] values (μM) of enzyme inhibition of compounds **39** and PACMA31 against PDIA3 and PDIA6

n=***
40
PDIA1:0.63 ±0.01μM
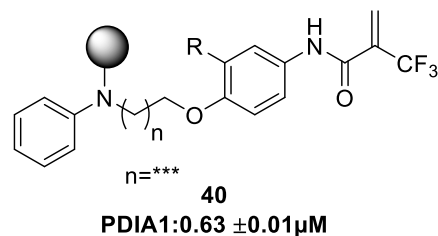
Compound	PDIA1 (PDI)	PDIA3 (ERp57)	PDIA6 (ERp5)
40	0.63 ± 0.01	1.13 ± 0.25	5.17 ± 0.31
PACMA31	8.10 ± 0.90	28.09 ± 1.94	>40

[a] Data are provided from three independent experiments.

Compound **40** exhibited potent cytotoxicity against GBM cells

(A)

(B)
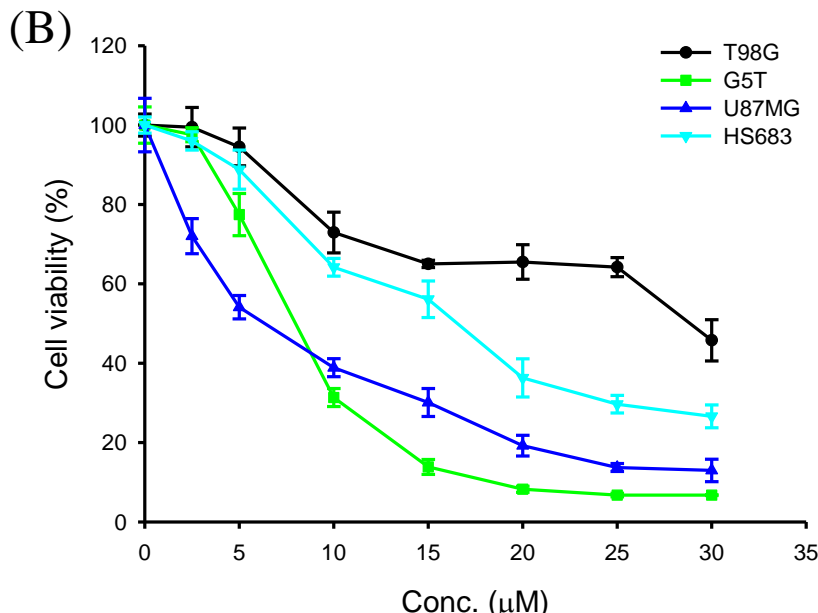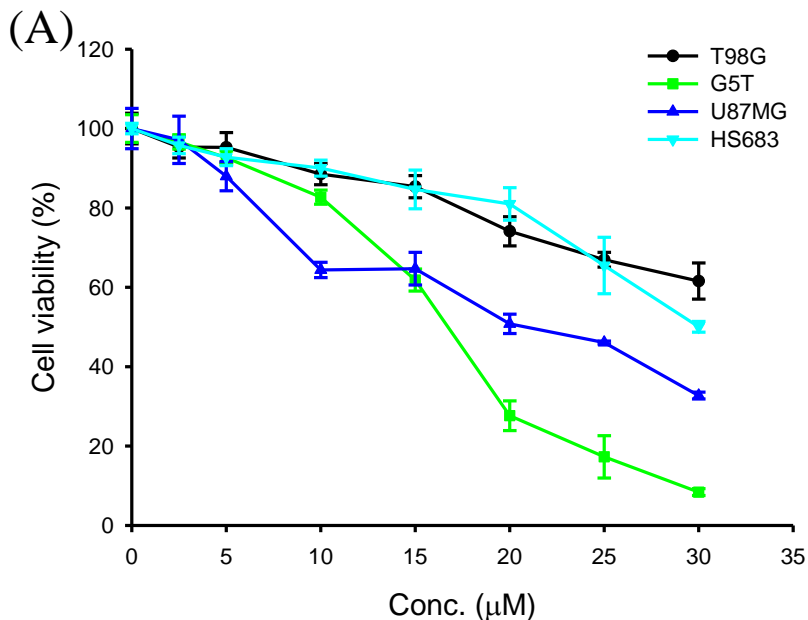
(C)

Compound	Cell lines (IC$_{50}$, μM)			
	T98G	G5T	U87-MG	HS683
27a	>30	16.7	21.6	>30
40	28.4	10.6 ± 1.2	10.0 ± 0.8	17.9
TMZ	ND	630.1 ± 18.2	627.2 ± 80.9	ND

Figure 7. Glioma cells were seeded in 24 well for 24 h, and then treated with 0~30 μM **27a** (A) or **40** (B) for 72 h. The cell viability were analyzed using MTT assay. The IC$_{50}$ of each cell line were calculated (C).

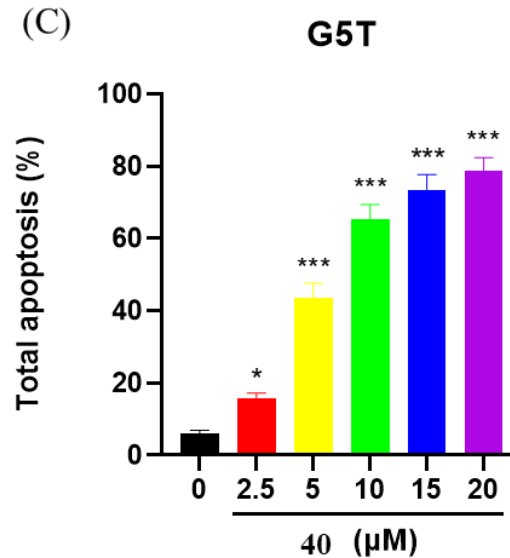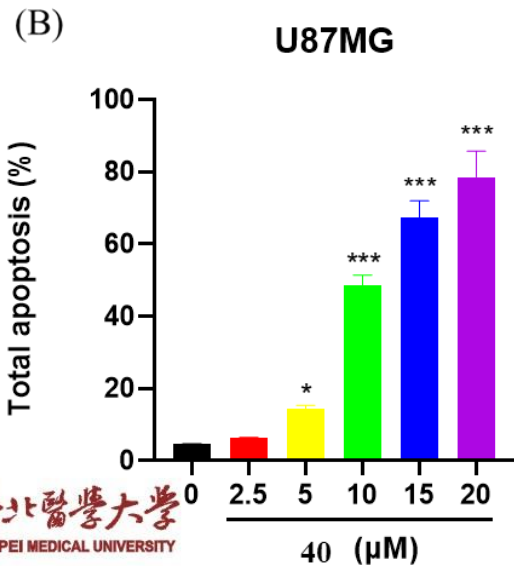# Compound **40** induced cell apoptosis in GBM cell lines

Figure 8. The effect of compound **40** induced cell apoptosis and accumulation of cell cycle in subG1 phase against U87MG and G5T glioma cell lines. (A) Both U87MG and G5T cell lines were treated with compound **40** at 0, 2.5, 5, 10 15, 20 and 25 μM for analyzing the total apoptosis rate by flow cytometry. (B, C) The statistical analysis of total apoptosis rate for U87MG (B) and G5T (C) cell lines after treating various dose of compound **40**. *p < 0.05, **p < 0.01, ***p < 0.001 vs. control.

Compound **40** induced cell apoptosis and accumulation of cell cycle in subG1 phase against U87MG and G5T glioma cell lines
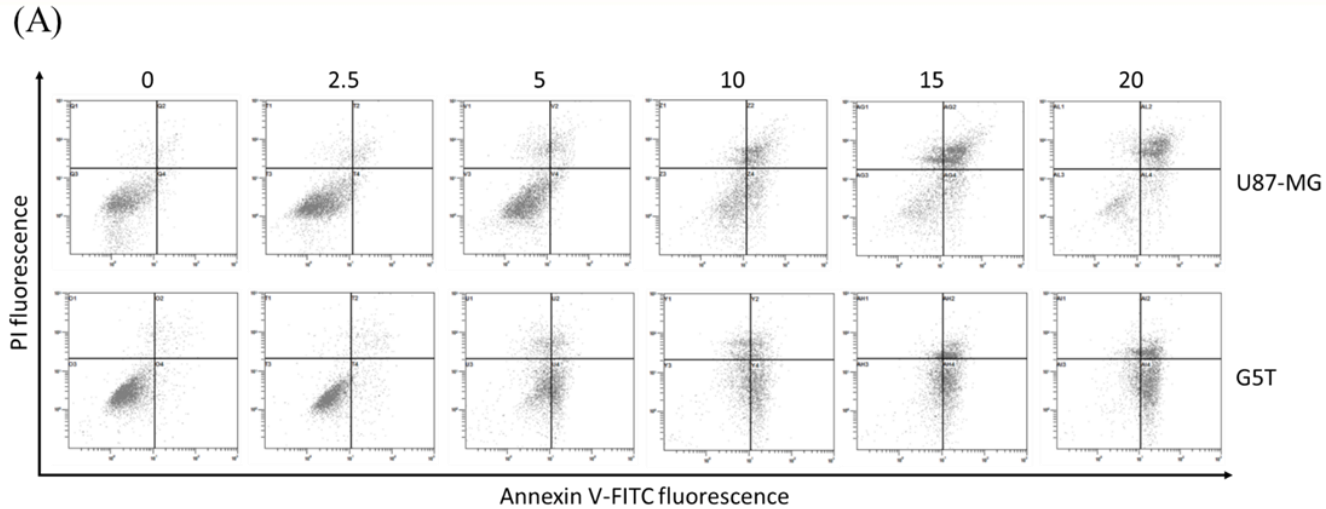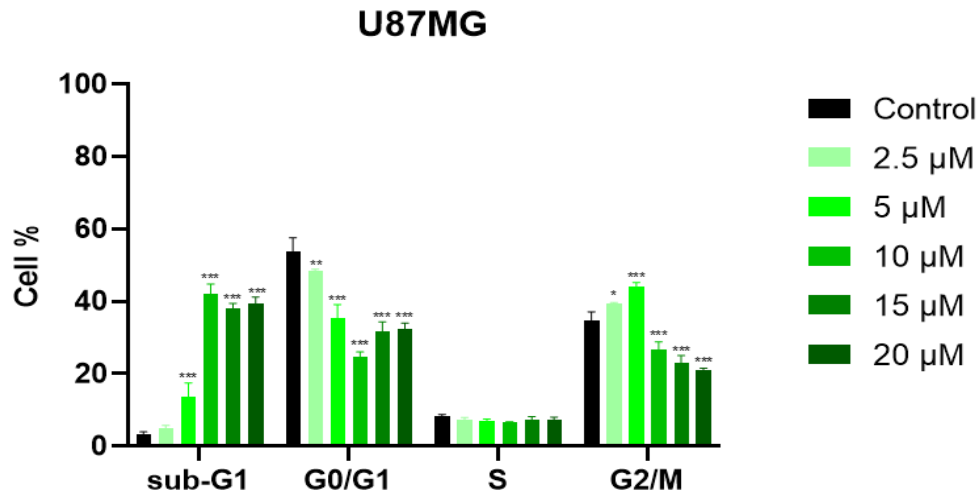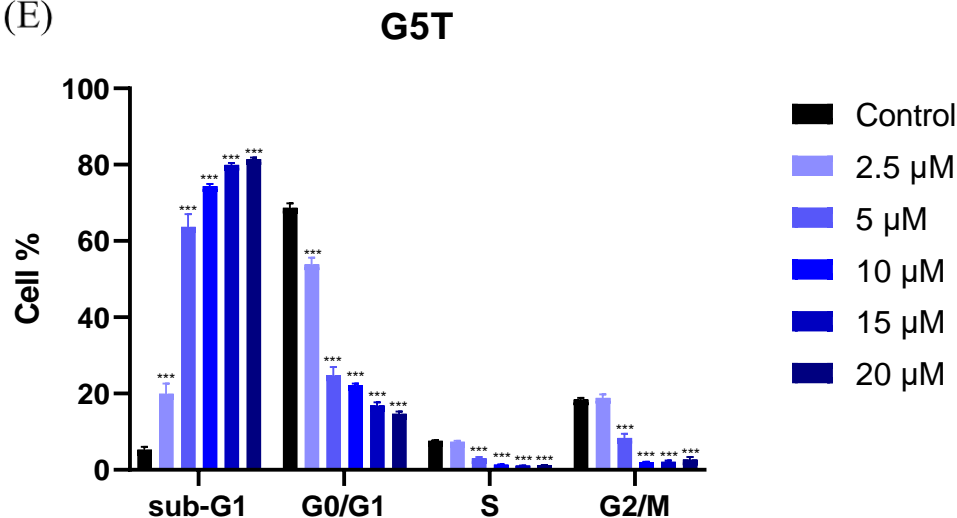

(D) U87MG

Figure 8. The effect of compound **40** induced cell apoptosis and accumulation of cell cycle in subG1 phase against U87MG and G5T glioma cell lines. (E, F) The statistical analysis of cell cycle distribution for U87MG (E) and G5T (F) cell lines after treating various dose of compound **40**. The data were obtained from three experiments. *p < 0.05, **p < 0.01, ***p < 0.001 vs. control.

(E) G5T

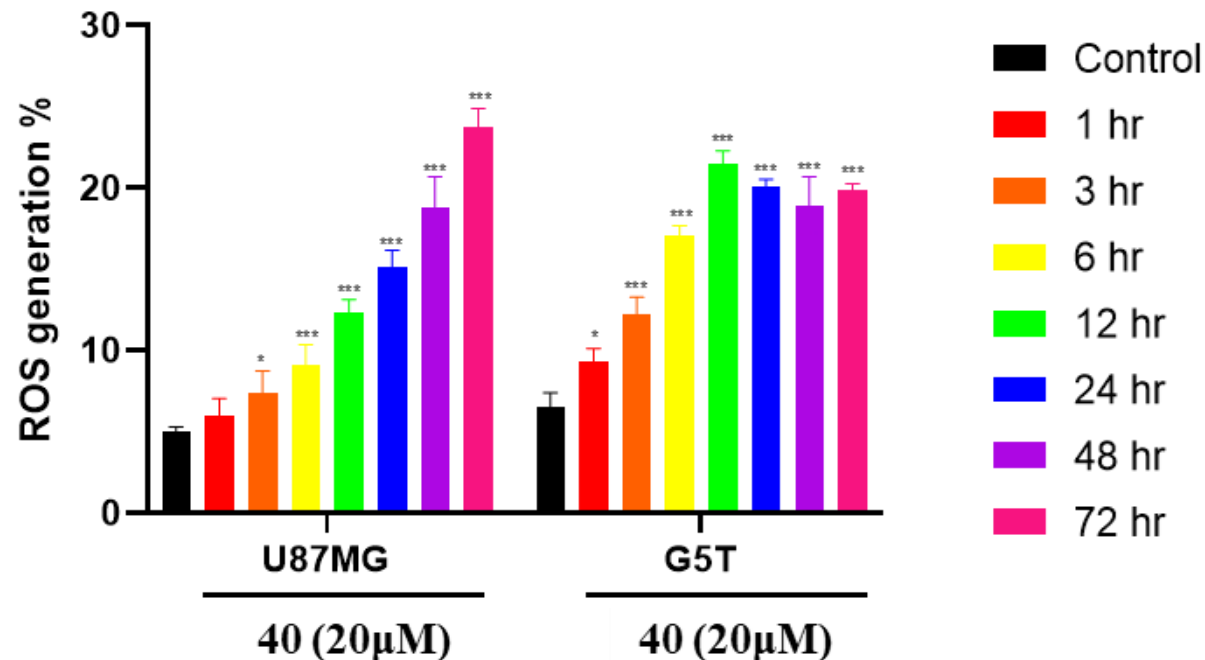# Compound **40** increased ROS generation in GBM cell lines
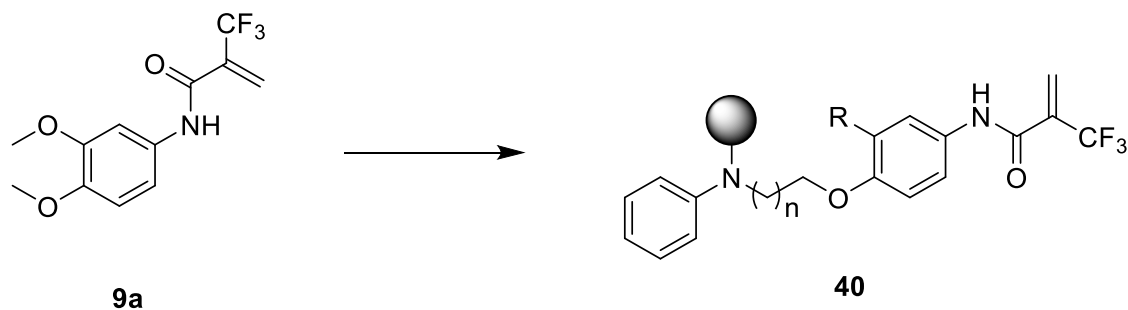

Figure 9. The effect of compound **40** enhanced ROS production in U87MG and G5T cells. The statistical analysis of ROS production for cells staining with the ROS probe. The data were obtained from three experiments. $*p < 0.05$, $**p < 0.01$, $***p < 0.001$ vs. control.

Compound **40**, combined with TMZ, displayed a synergistic effect against GBM cells

Conclusion

9a → 40
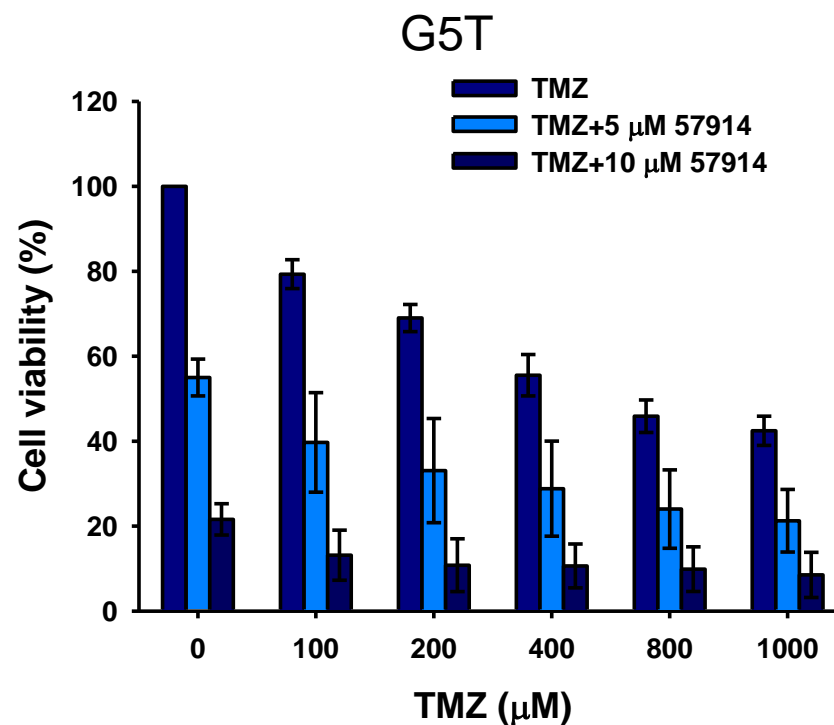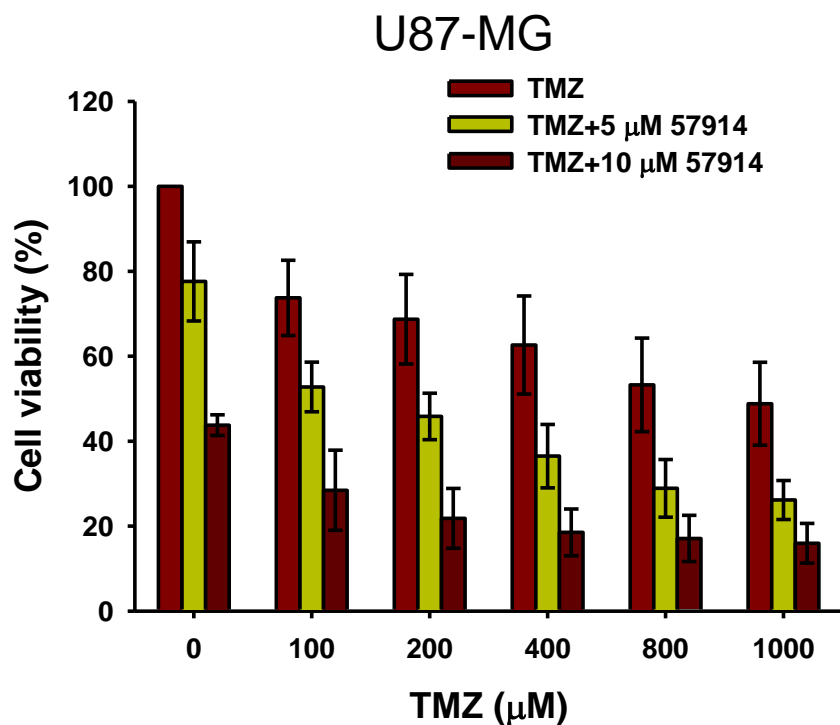
- Compound **40** exhibited potent inhibition of PDIA1 with an IC_{50} value of 0.63 ± 0.01 μM.

- Compound **40** inhibited cell proliferation against U87MG and G5T glioma cell lines with an IC_{50} value of 10.0 ± 0.8 μM and 10.6 ± 1.2 μM, respectively.

- Compound **40** induced apoptosis and increased ROS generation in U87MG and G5T glioma cell lines.

- Compound **40** produced synergistic effect with TMZ, resulting in enhancing cytotoxicity of TMZ against GBM cell lines.

ACKNOWLEDGMENTS

ACKNOWLEDGMENTS

Thank you for your attention